

8.3 Problems in Propulsion System Integration

W. Henderson and J. Runckel
NASA Langley Research Center

Problems in Propulsion System Integration

The problems associated with propulsion system integration are related to the placement of the engine on the airframe. The complexity of the problem, and the associated drag, depends on the area where the power plant is located--as indicated on Figure 1.

Wing installations can consist of nacelles located under or over the wing or propulsive wing concepts. The exhaust stream can produce either favorable or unfavorable induced effects on lift and drag.

The fuselage could contain lift engines or adjacent nacelles which produce interference drag and the hot exhaust can have detrimental effects on the structure.

The afterbody with buried engines is a particular problem with military aircraft since a large portion of the drag occurs in this region.

Reverse thrust on rear mounted engines can pose plume impingement problems on stabilizing surfaces.

I will touch briefly on several of the areas indicated on Figure 1.

The main problems with jet-engined aircraft are with the induction system and the exhaust system and the effects on configuration performance consisting of mutual interferences between the propulsion system and the airframe.

Interference effects are usually evaluated first by looking at the isolated components of the propulsion system and then with the system integrated into the airframe. I would like to present some recent NASA work on jet engine components which can influence the related aircraft drag areas.

Preceding Page Blank

FOREBODY
PROPELLER/ENGINE, INLETS
WING
FLOW FIELD/NACELLE INTERFERENCE
INDUCED EFFECT - LIFT AND DRAG
FUSELAGE
INTERFERENCE DRAG
EXHAUST EFFECTS
INDUCED PRESSURES - STATIC/DYNAMIC-ACOUSTIC
INDUCED TEMPERATURES
AFTERBODY
POWER EFFECTS ON DRAG
NOZZLE/AIRCRAFT CLOSURE
REVERSE THRUST
EMPENNAGE
PLUME EFFECTS ON STABILITY
VERTICAL TAIL ENGINE INSTALLATION

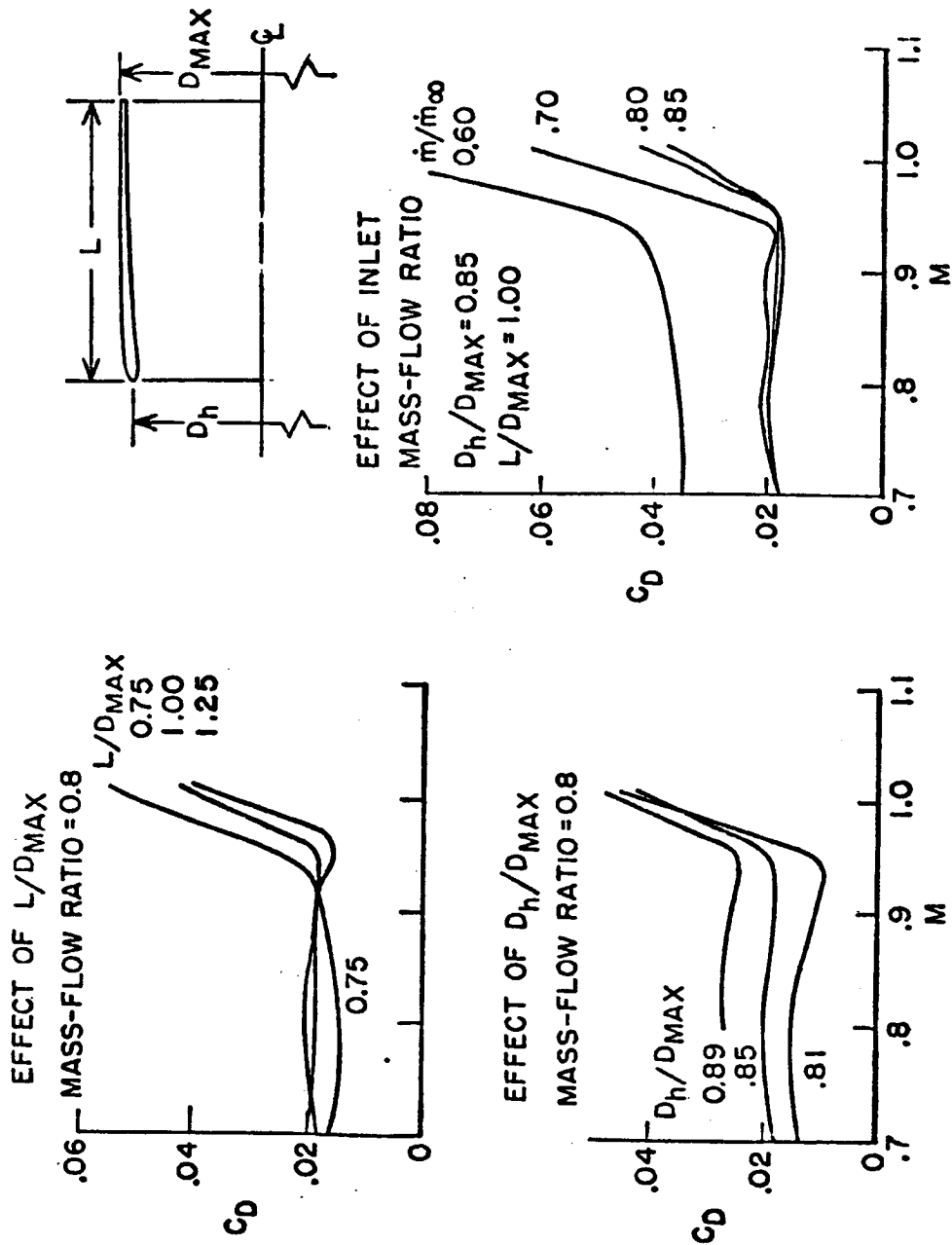
Figure 1. Influence of Propulsion System on Airframe Aerodynamics

Nose Inlets

The early work on NACA inlets has recently been extended to higher Mach numbers and updated for geometries corresponding to the mass flow requirements of high bypass rotor fan engines. Figure 2 shows the experimental results of the investigation. The variables were fineness ratio, inlet highlight to maximum diameter ratio mass flow and angle of attack. The upper left chart in Figure 2 shows the effect of fineness ratio at a constant mass flow ratio of 0.8. The short inlets are best at lower speed but drag rise Mach number increases with fineness ratio. Figure 2 shows the effect of diameter ratio—drag increases as the inlet is opened up but the critical Mach number is extended. The right side of the figure shows the effect of mass flow ratio variation where reductions in drag and increases in the knee of the drag curve increase with increased inlet mass flow ratio. These data were obtained from force balance measurements and the drag coefficient is based on the maximum cross-sectional area.

Reference

An Investigation of Sever NACA 1-Series Axisymmetric Inlets at Mach Numbers from 0.4 to 1.29. Richard, J. Re. NASA TM X-2917, March 1974.



16-FT. T.T. BR. HSAD LRC 9-72

Figure 2. Nose Inlets at Transonic Speeds

Inlet Instrumentation Prediction

Pressure distribution measurements were also obtained during the inlet investigation. Figure 3 shows a comparison of a theoretical prediction with an experimental pressure distribution. The measured pressure coefficients are indicated by the circular symbols for both the outer cowl and on the inside of the inlet. Data are for an inlet with highlight to maximum diameter ratio of 0.85 and fineness ratio of 1.0 at 0.7 Mach number and a mass-flow ratio of 0.87. The calculated pressure distribution using a stream tube curvature theory developed for NASA is shown by the line. This theory accounts for both the internal and external flow field at the inlet and can also be used to calculate the pressure distribution on afterbodies with a jet exhaust. The agreement is very good with only a slight miss on the lip peak suction pressure.

Reference

Analytical Method for Predicting the Pressure Distribution about a Nacelle at Transonic Speeds. J. S. Keith, D. R. Ferguson, C. L. Merkle, P. H. Heck and D. J. Lahti. NASA CR-2217, July 1973.

○ 16' T DATA (8 CONFIGURATIONS M = .4 - 1.2 AUG '71)
 — THEORY (G. E. CO. CONTRACT FOR TRANSONIC NACELLES)

NACA 1-85-100
 MACH NO. = .7 FLOW RATIO = .87

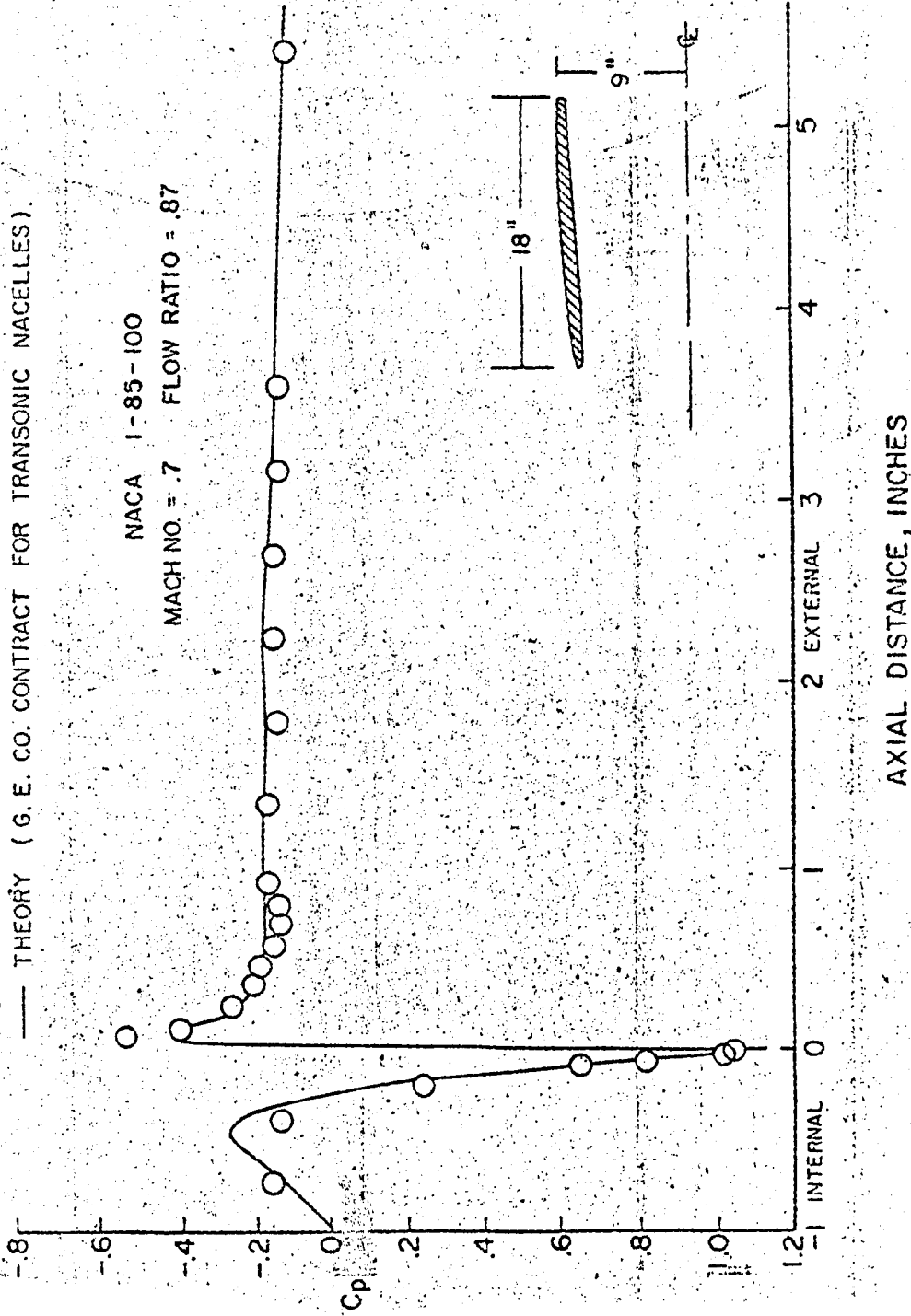


Figure 3. Transonic Inlet Results

Nozzle Boattail Drag

(We have also developed an extensive data base on the drag characteristics of boattailed afterbodies.)

A series of nozzle boattail configurations has been investigated at subsonic and transonic speeds to determine the pressure drag for various shapes, fineness ratios and closure ratios which should be applicable to several types of jet and fan engines. Shown in Figure 4 are samples of data for circular arc boattails from a program where fineness ratio varied from 0.8 to 2.0 and closure ratio from 0.5 to 0.7. The variation of drag with Mach number is shown for a short steep boattail on which the flow separated and a higher fineness ratio boattail with attached flow. Experimental data is indicated by the symbols and theoretical predictions by the lines. For attached flow the prediction is reasonable until supercritical velocities are approached. For the separated flow case, however, existing theory is inadequate and further work is being done to improve the situation. The limitations to existing theory include transonic flow and imbedded shocks, separated flow regions and inadequate modeling of the jet exhaust to include entrainment effects.

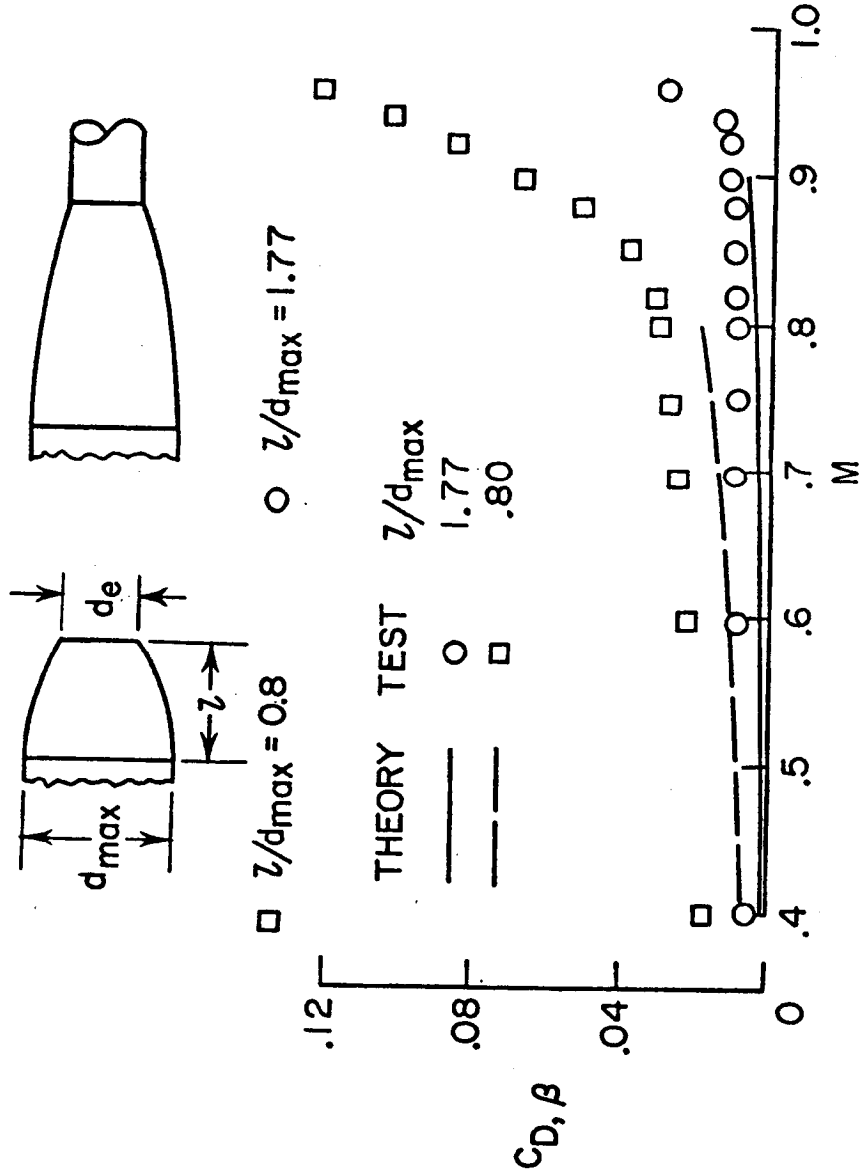


Figure 4. Nozzle Boattail Drag Shape, Fineness Ratio, Closure Ratio = 0.5

Propulsive Wing Installation

Figure 5 shows an example of a propulsion system completely integrated into the wing. The configuration is a propulsive wing utilizing four tip-turbine driven fans. The wing fans, oriented in the axial direction, induce air into the leading edge of the wing and exhaust it at the trailing edge. Either lift and/or axial thrust are obtained by means of a slipstream deflection and modulation system. In the cruise mode, variable angle flaps aid in the control of fan flow direction as well as provide expansion surfaces for the two-dimensional turbine exhaust flow from the gas generator--similar to a jet flap concept. Although the wing was geometrically thick (thickness to chord ratio of 25 percent), aerodynamically it was relatively thin as indicated by the drag rise which occurred at a Mach number of 0.85.

Reference

Longitudinal Aerodynamic and Propulsion Characteristics of a Propulsive-Wing V/STOL Model at High Subsonic Speeds. Leland B. Salters, Jr., and James W. Schmeer. NASA TMX-2693. January 1973.



Figure 5. Example Propulsive W Installation

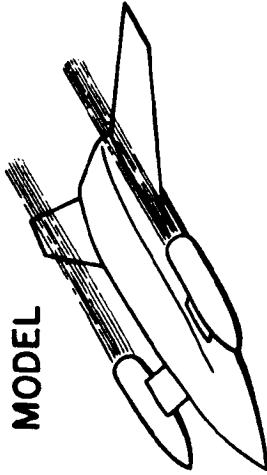
Blowing Over the Wing

Upper-surface blowing propulsive lift concepts have shown a potential for attaining good low-speed high-lift performance with lower noise levels because of the shielding afforded by the wings between the jet related noise and the ground. Only preliminary work has been done on the effects of propulsive lift cruise performance. Shown on Figure 6 are results from an experimental and analytical investigation to determine the effects of forward mounted jets blowing over a wing. The model had a low aspect ratio wing and forces were measured on the wing-afterbody portion. The nacelles were located forward and above the wing. The analytical method represented the wing lifting surface with a lattice of horseshow vortices and simulated the effects of the exhaust plume with a line sink-source distribution located on the axis of the jet. The theory accurately predicted the variation in interference lift due to the jet flow for Mach numbers of 0.4 to 0.7. The theory also predicted the reduction in induced drag indicated by the data. The favorable increment in induced drag increases with both the ratio of jet velocity to free stream velocity and wing lift coefficient. The plots on the right side of Figure 6 show that the theory correctly predicts both the increase in lift and the reduction in induced drag coefficient.

References

1. Exploratory Investigation at Mach Numbers from 0.40 to 0.95 of the Effects of Jets Blown Over a Wing. Lawrence E. Putnam. NASA TND-7367, November 1973.
2. An Analytical Study of the Effects of Jets Located More than One Diameter Above a Wing at Subsonic Speeds. Lawrence E. Putnam. NASA TND-7754, August 1974.

WIND TUNNEL MODEL



THEORETICAL MODEL

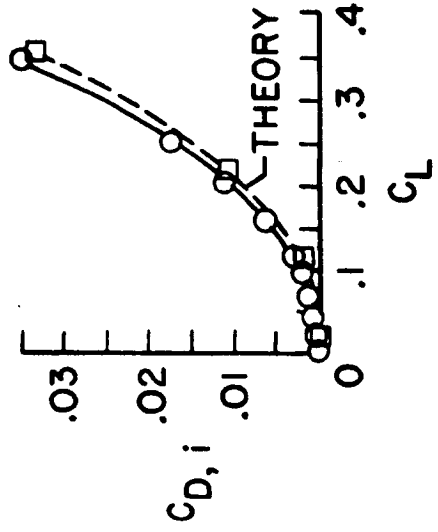
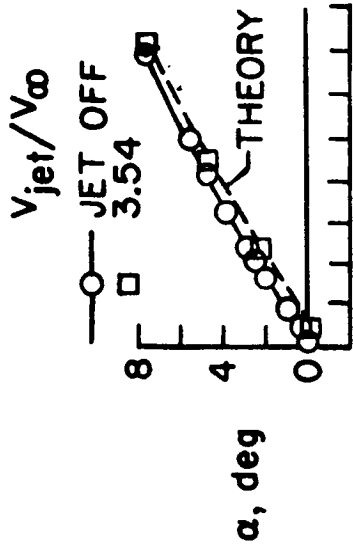
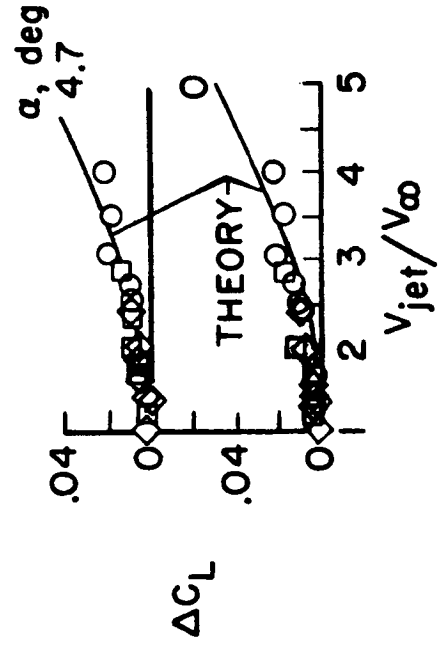
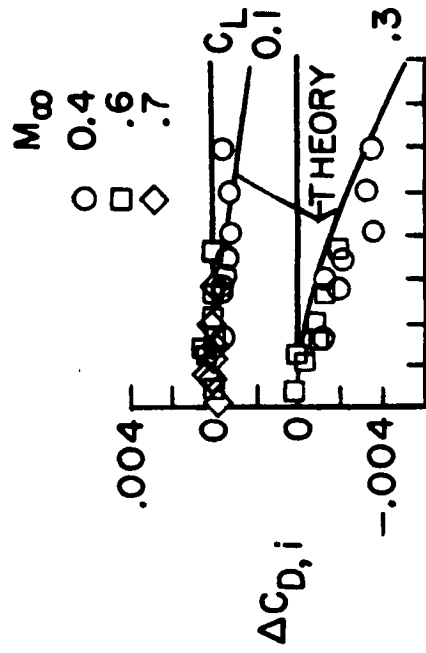
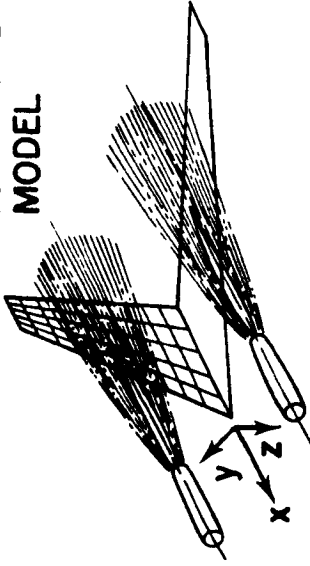


Figure 6. Jets Blowing Over Wing

Induced Drag Reduction By Over-the-Wing Blowing

The theoretical method we developed was also used to correlate some existing data on blowing over the wing. Fokker VFW research results presented at a 1974 AGARD meeting are shown in Figure 7. The engine-nacelle configuration is shown in the upper right hand corner and was located above and forward of the wing. The plot shows the change in induced drag coefficient for jet off and a jet to free stream velocity ratio of about 7.5 by the data points; circles for cruise, squares for climb values of left coefficient. The theory calculations are indicated by the broken lines, and again, the predictions agree well with the data. The actual values of velocity ratio required for climb and cruise are indicated by the broken bars. The reductions in induced drag at climb are still substantial and some benefits still occur at cruise.

Reference

Airframe-Engine Interaction for Engine Configurations Mounted Above the Wing. Part 1: Interference Between Wing and Intake/Jet, by G. Kreng. In: AGARD Conference Proceedings No/SD on Airframe/Propulsion Interference AGARD-CP-150, September 1974.

$M_{CRUISE} = 0.6$

THEORY EXPERIMENT

--- ---
 O □

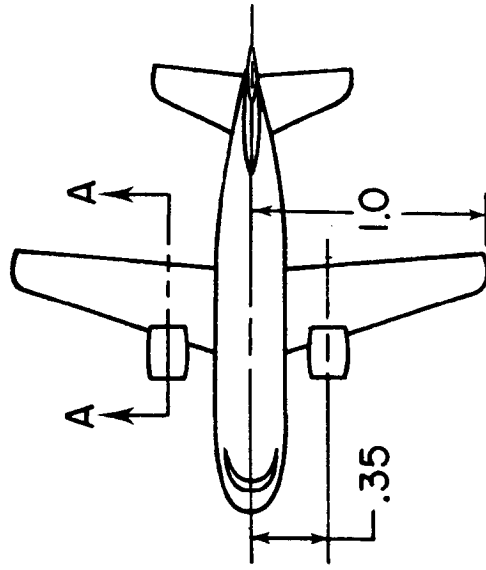
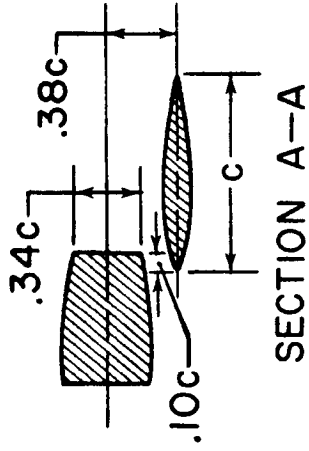
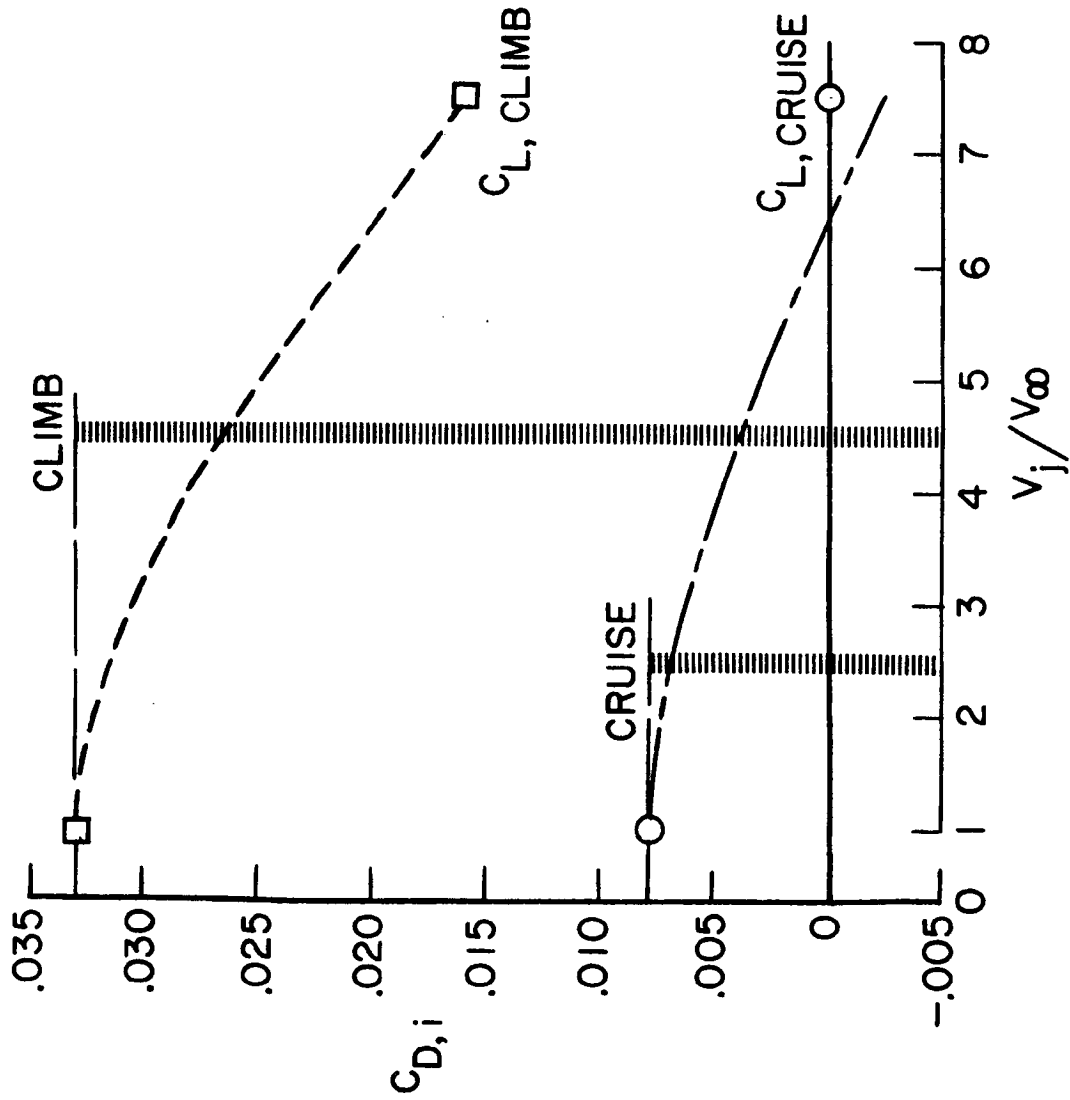


Figure 7. Induced Drag Reduction by Over-the-Wing Blowing

Propulsion/Aero Effects on Cruise Efficiency

These exploratory results have encouraged us to look at the performance benefits that may be possible with transport configurations during cruise flight.

Figure 8 illustrates a current program aimed at determining the cruise efficiency of highly integrated propulsion systems. A powered model of a basic transport configuration is under construction which will allow various types of engine locations on the wing to be studied and performance comparisons to be determined. Three types of engine installations will be considered: conventional under the wing pylon mounted nacelles; over the wing nacelles; and a blended upper surface blowing configuration. An internal balance system will measure all forces on the model including the thrust. The types of propulsion systems are shown on the right and consist of flow through nacelles, blown nacelles with air jets and turbofan simulators. These simulation systems will provide aerodynamics model data comparisons, the jet induced lift and drag increments and the contribution of the inlet flow simulation on the flow field.

ENGINE LOCATION



BLENDDED USB

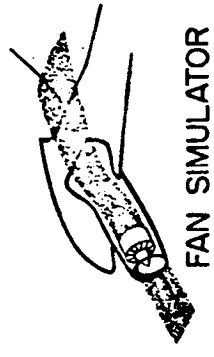


CONVENTIONAL

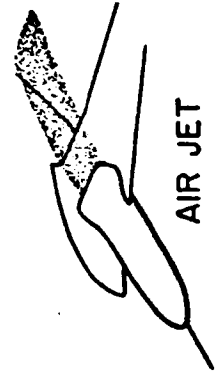


OVER THE WING

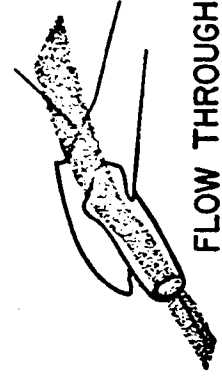
PROPULSION SIMULATION



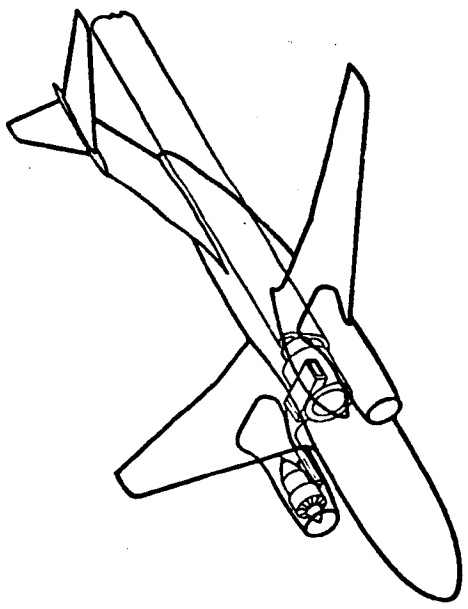
FAN SIMULATOR



AIR JET



FLOW THROUGH



BASIC POWERED MODEL

Figure 8. Propulsion/Aero Effects on Cruise Efficiency

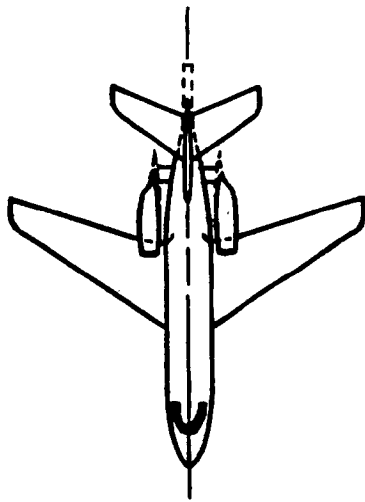
Fuselage Mounted Nacelles

The information presented on Figure 9 shows the drag increments that can be expected with an aft fuselage mounted nacelle configuration. The model represented a small twin-jet business transport and was investigated with various nacelle arrangements. The circular symbols show the variation of drag coefficient with Mach number for the basic wing-fuselage-empennage. Addition of the fuselage mounted pylons and nacelles increase the drag to the level shown for the square symbols. The calculated skin friction of the pylon nacelle combination when added to the baseline configuration would give a drag variation as indicated by the top line of the cross hatching. The installation penalty for the propulsion system package is small in this case and there is some beneficial interference at the highest speeds. Even lower values of the complete aircraft drag can be obtained by the alterations to the nacelle installation as indicated on the right side, where decreases in drag due to changing longitudinal location, increasing incidence angle and cant angle and changes in the effective area distribution in the fuselage nacelle region are shown.

References

Effects of Aft-Fuselage-Mounted Nacelles on the Subsonic Longitudinal Aerodynamic Characteristics of a Twin-Turbojet Airplane. Lawrence E. Putnam and Charles E. Trescot, Jr. NASA TND-3781, December 1966.

C.S.



**INTERFERENCE DRAG
REDUCTIONS**

**DRAG
COUNTS**

- LONGITUDINAL LOCATION 2-5
- INCIDENCE ANGLE 3-10
- CANT ANGLE 3-4
- NACELLE AND PYLON EXTENSION 3-8

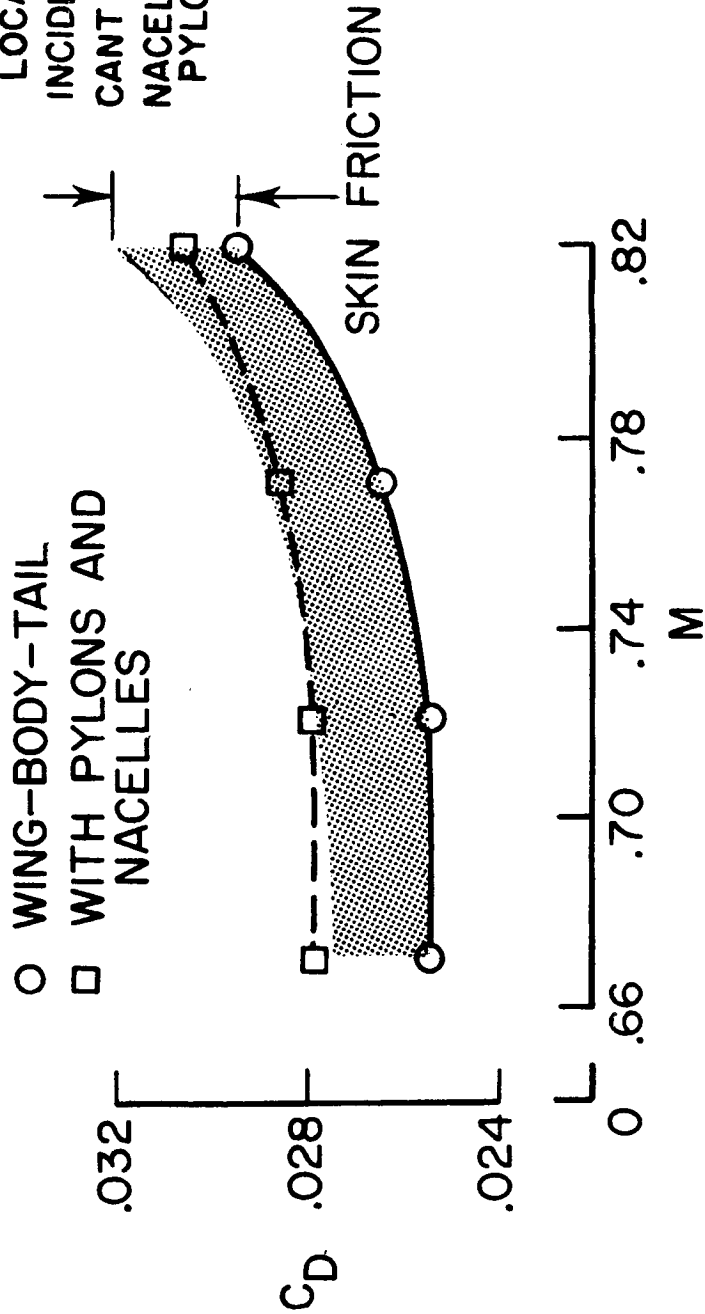


Figure 9. Aft Fuselage-Mounted Nacelle Configuration - $C_L = 0.25$

In-Flight Thrust Reversal

Shown in Figure 10 is a 1/15-scale model of the Gulfstream II mounted in the Langley 16-foot transonic tunnel. The model was modified for powered model testing by splitting the fuselage aft of the wings and measuring forces on the rear end. The objective of this investigation was to increase the drag to make the vehicle suitable for a Shuttle Training Aircraft. This was accomplished by use of both speed brakes and in-flight cascade type thrust reversers. Figure 10 shows flow through nacelles which were faired over for the reverse jet thrust simulation. In-flight thrust reversal was enhanced by both the reverse thrust vector and drag produced by low pressures on the aircraft behind the reverser. As reverse thrust power level increased and speed decreased, the exhaust plume got progressively closer and in some cases enveloped the horizontal tail. This resulted in a decrease in tail contribution to stability and control effectiveness as well as increased trim changes and horizontal tail dynamics. Reverse thrust plume visualization was obtained by injecting water into the exhaust and verified the force data. Exhaust plume impingement can be a problem with conventional aircraft at high angles of attack.

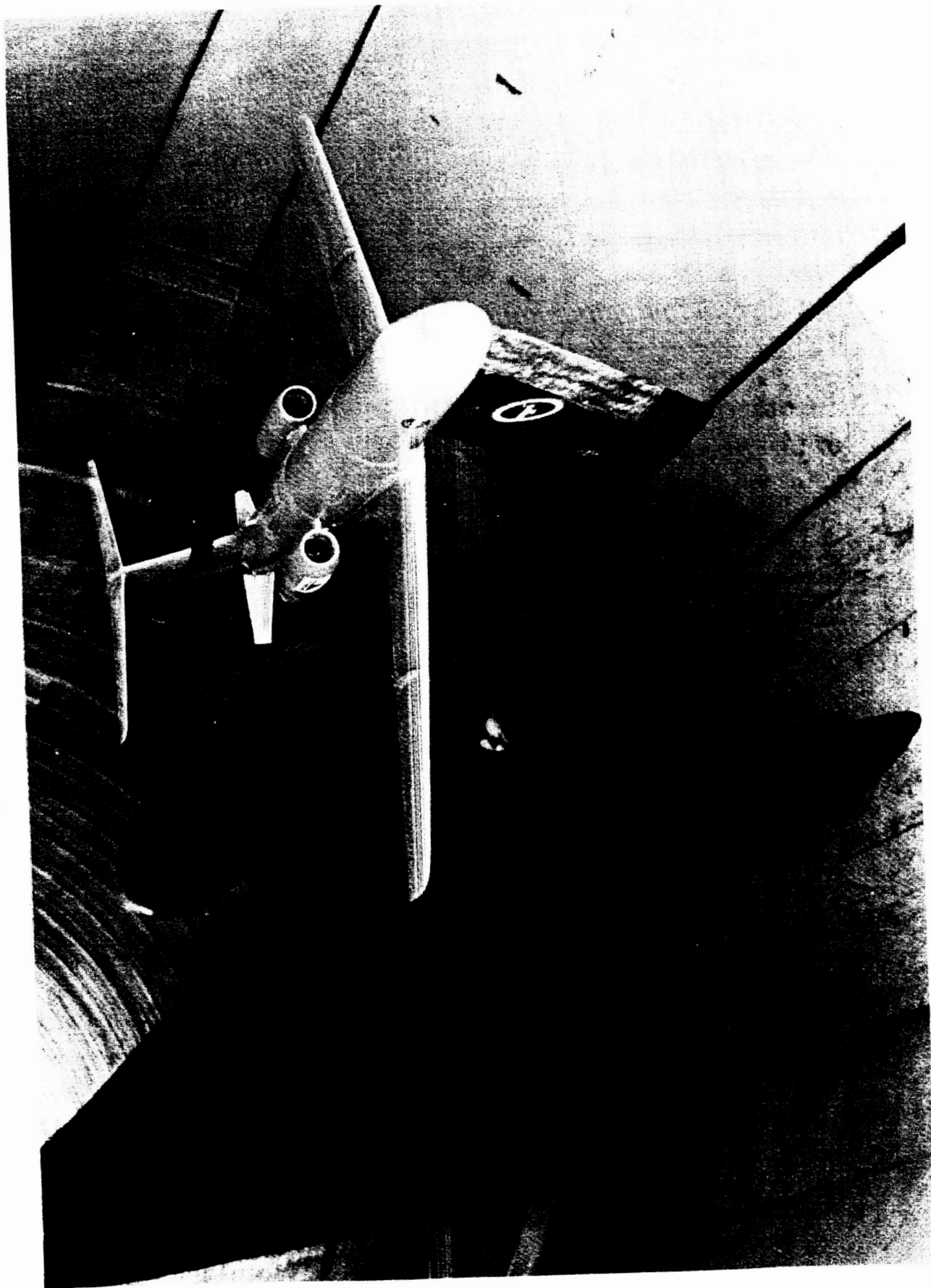


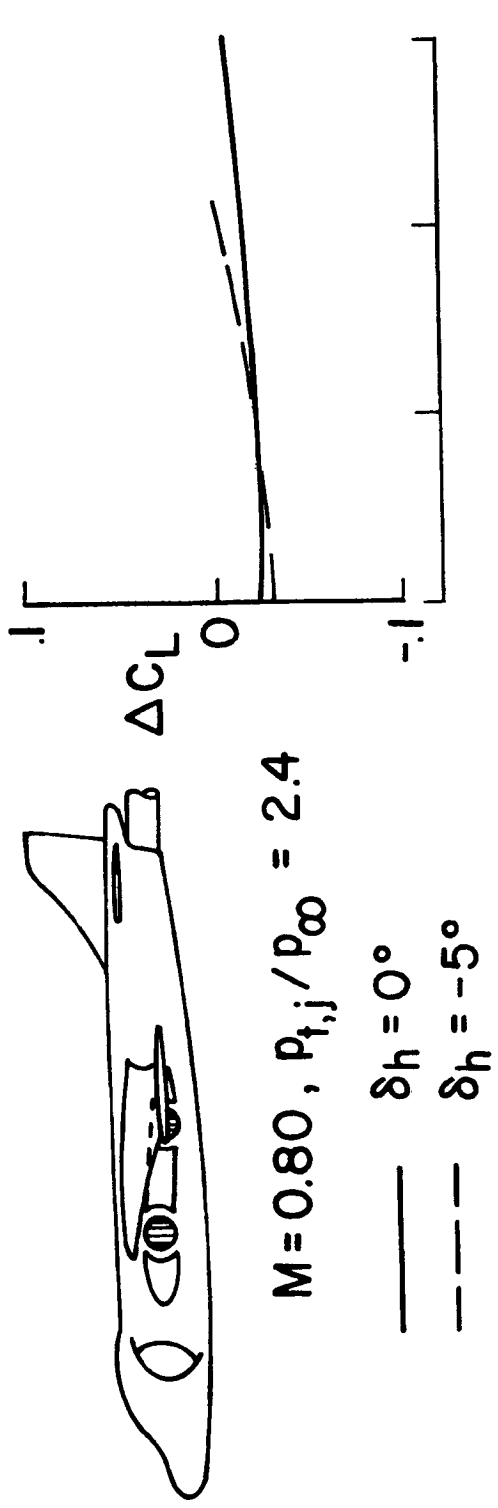
Figure 10. In-Flight Thrust Reversing System

Jet Effects on Aero Characteristics

An example of jet interference effects on complete aircraft aerodynamics is shown in Figure 11. (The testing techniques for complete powered models are usually more difficult because of support system and inlet simulation problems.) This single-engine four-jet V/STOL type aircraft was tested with an injection propulsion system. The exhaust nozzles, two on each side are located close beneath the wing. The data represent the change in aerodynamic coefficients caused by a change from power-off to power-on flight. Results are shown as a function of angle of attack for $M = 0.8$ and horizontal tail deflections of 0° and 5° . In this case, jet effects are not large. Jet operation decreased lift and drag and increased pitching moment. When referred to the absolute values of the coefficients required in flight, these increments represent a reduction in lift and drag respectively, of about 5 and 10 percent. Although the magnitude of pitching moment coefficient increased due to simulated jet operation, only slight changes in model longitudinal stability were found.

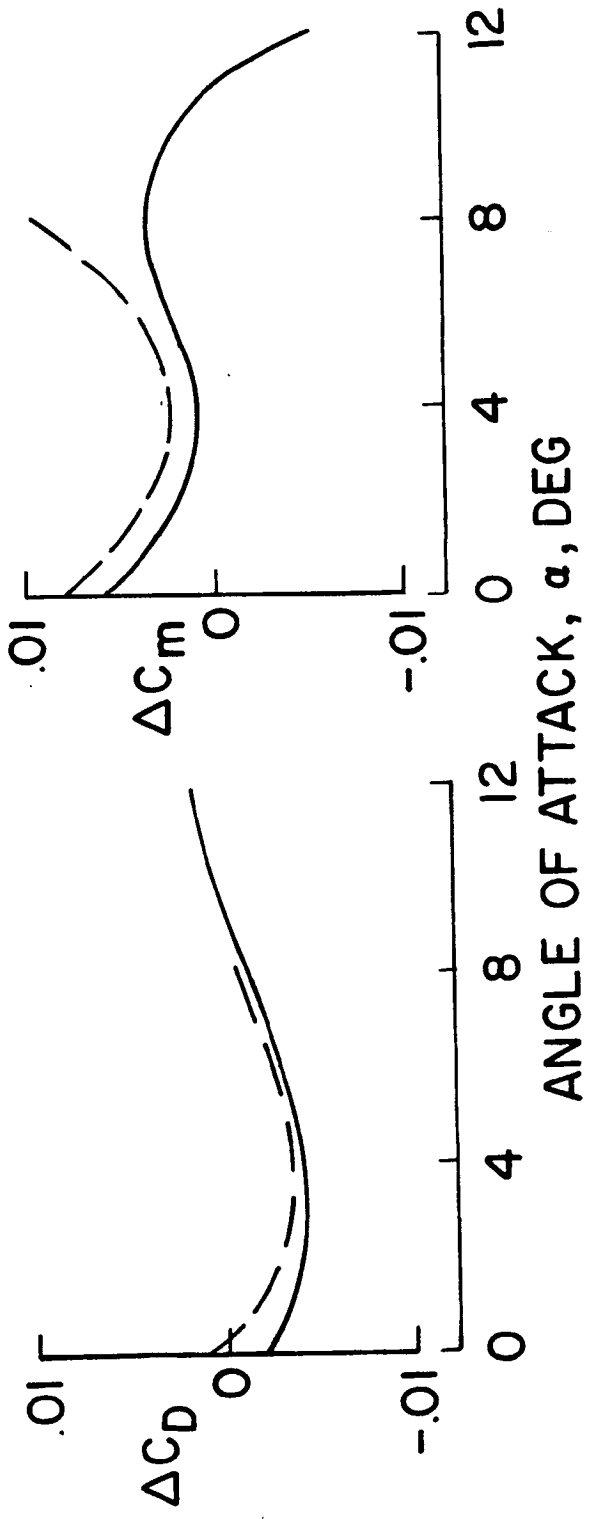
I have attempted to illustrate some problems that may be associated with the integration of the power plant into the airframe. The examples illustrated are probably much more severe than those occurring with general aviation aircraft.

NASA has the experimental facilities and is developing the analytical tools which will aid in the reduction of interference drag and provide guides for the best ways to incorporate the power plant into the aircraft.



$M = 0.80, P_{t,j} / P_\infty = 2.4$

— $\delta_h = 0^\circ$
 - - $\delta_h = -5^\circ$



ANGLE OF ATTACK, α , DEG

Figure 11. Jet Effects on Aero. Characteristics
 (Jet On - Jet Off)